Application of Boundary-Fitted Coordinate System to the Wave Propagation in a Circular Channel
만곡 수로에서의 파랑 전파 예측을 위한 경계 고정 좌표계의 적용

Jung Lyul Lee*

이 정 렬*

Abstract ☐ The paper deals with the application of Boundary-Fitted Coordinate System (BFCS) to the two wave models of parabolic and hyperbolic types developed on a rectangular grid system. Since the BFCS conforms the boundaries of the region in such way that boundary conditions or calculation process can be accurately represented, improvement in predicting the wave fields can be achieved. The numerical results show a good agreement with the analytical results for either waves propagating or reflecting along a circular channel of constant depth. Simulation of reflecting waves in a parabolic wave model is accomplished by the backward calculation as if waves approached at the cross wall take a turn in the opposite direction and propagate against a channel.

Keywords : boundary-fitted coordinate, wave propagation, wave reflection, parabolic model, hyperbolic model, circular channel

要　旨 : 본 논문은 경계처리 및 계산과정에 있어서 좀더 개선된 파랑 예측이 보장되도록 기존의 정방형 좌표계에서 수립된 포물선형 및 쌍곡선형 파랑 모델을 경계고정좌표계에 적용하였다. 일정 수심의 만곡 수로를 따라 진행 및 반사하는 파랑에 대한 이론해와 비교하여 수치 모델 결과는 모두 만족할만하였다. 포물선형 모델의 반사 파랑 모의는 반사물에 접근한 입사파를 다시 외해 경계 쪽으로 역계산하여 수행된다.

핵심용어 : 경계 고정 좌표, 파랑 전파, 파의 반사, 포물선형 모델, 쌍곡선형 모델, 만곡 수로

1. INTRODUCTION

The parabolic approximation method in solving wave phenomena is known to have a great merit as time-saving method. However, the method shows a disagreement for the wide angle and behind the structures since the numerical scheme used proceeds grid by grid along a main axis. When waves propagate through a turning channel, this disagreement also occurs due to the turning angle of wave propagation and the zigzag boundaries on the Cartesian methods. The improvement for this disagreement is accomplished by using the boundary-fitted grid system to a complicated region. The interest in numerically-generated, Boundary-Fitted Coordinate Systems (BFCS) has arisen from the need for conforming the boundaries of the region in such way that boundary conditions can be accurately represented.

Several investigators such as Liu and Boissevain (1988), Kirby (1988), and Dalrymple and Kirby (1994) have employed the BFCS to propagating wave fields; Liu and Boissevain (1988) applied a non-conformal transformation to waves between two breakwaters. Kirby (1988) examined Liu and Boissevain's model by

---

*성균관대학교 토목환경공학과 (Department of Civil and Environmental Engineering, Sungkyunkwan University, Suwon Science Campus, Suwon 440-746, Korea)

constructing the parabolic approximation in the transformed space. Recently, Dalrymple and Kirby (1994) developed the forward-propagation equations for Fourier-Galerkin and Chebyshev-Tau models in conformal domains, and compared the results to the exact solutions of waves in a circular channel. There was another recent work on wave propagation through circular rubble-mounded jetties done by Melo and Gobbi(1998). In this study we develop two wave models by mapping the wave equations of hyperbolic and parabolic types through the boundary-fitted coordinate transformation and compare the model results to the exact solutions of waves either propagating or reflecting in a circular channel with a constant depth.

2. WAVE EQUATION

In the past two decades, prediction of nearshore waves took a new dimension with the introduction of the mild slope equation by Berkhoff (1972) which is capable of handling the combined effects of refraction and diffraction. Since then significant progress has been made in computational techniques as well as model capabilities, notably by Radder (1979), Copeland (1985), Ebersole *et al.* (1986), Yoo and O'Connor (1986), Madsen and Larsen (1987), Panchang (1988), and Dalrymple et al. (1989). However, no single model has been proven to be perfect or has clearly outperformed the others at present. The mild-slope equation of Berkhoff (1972) is expressed in terms of instantaneous water surface velocity potential, ϕ as

$$\nabla \cdot (CCg \nabla \phi) + k^2 CCg \phi = 0 \qquad (1)$$

Writing $\Phi = \phi \sqrt{(CCg)}$ allows Eq. (1) to be cast into the form of a Helmholtz equation. Under the assumptions of slowly varying depth and small bottom slope, the equation for Φ may be approximated as (Radder, 1979),

$$\nabla^2 \Phi + k_c^2 \Phi = 0 \qquad (2)$$

where $k_c^2 = k^2 - \nabla^2 (CCg)^{0.5}/(CCg)^{0.5}$. Starting from Eq. (2), governing equations of parabolic and hyperbolic

types on the boundary-fitted coordinate system will be derived. The present study is restricted to the case of constant depth.

3. BOUNDARY-FITTED COORDINATE SYSTEM

3.1 Coordinate System Transformation

The basic idea of a boundary-fitted coordinate system is to have some coordinate line coincident with each boundary segment, analogous to the way in which lines of constant radial coordinate coincide with circles in a cylindrical coordinate system. The coordinate system construction technique is based on the following Poisson generating equations.

$$\nabla^2 \xi = P, \ \nabla^2 \eta = Q \qquad (3)$$

where P and Q can be used to control the coordinate system as the source terms. In this study they are set to zero. The generating equations map the flow region in (x, y)-space to a computational region in (ξ, η)-space according to a transformation of the form

$$\xi = \xi(x, y), \ \eta = \eta(x, y) \qquad (4)$$

These methods are the extensions of the methods first successfully employed by Thompson *et al.* (1974). As usual the techniques are capable of treating arbitrary flow regions. This capability has been enhanced by the introduction of computational regions which are constructed from an arbitrary number of rectangles which are fit together so as to yield a suitable set of coordinates. Details on constructing such computational regions are given in Coleman (1982) which describes a program for generating such arbitrary transformations in two dimensions.

For computational purposes the generating system of Eq. (3) is transformed to the computational space by interchanging the dependent and independent variables. Then the transformed generating equations become

$$ax_{\xi\xi} - 2\beta x_{\xi\eta} + \gamma x_{\eta\eta} + J^2(Px_\xi + Qx_\eta) = 0$$
$$ay_{\xi\xi} - 2\beta y_{\xi\eta} + \gamma y_{\eta\eta} + J^2(Py_\xi + Qy_\eta) = 0 \qquad (5)$$

where

$$a = x_\eta^2 + y_\eta^2 \quad \beta = x_\xi x_\eta + y_\xi y_\eta \quad \gamma = x_\xi^2 + y_\xi^2$$

subscripts indicate differentiation. J is the Jacobian of transformation given as

$$J = x_\xi y_\eta - x_\eta y_\xi \tag{6}$$

The transformation can then be determined by solving Eq. (5) subject to appropriate boundary conditions. These conditions usually specify the dependence of x and y on ξ and η along the boundaries. Alternative conditions, such as the requirement that coordinate lines be orthogonal in physical space at a specified boundary, can also be applied.

3.2 Parabolic Model

In general curvilinear coordinates generated with $\nabla^2\xi=0$ and $\nabla^2\eta=0$, the non-conservative form of Laplacian operator can be written as

$$\nabla^2\Phi = \frac{1}{J^2}[x_\eta^2 + y_\eta^2)\Phi_{\xi\xi} - 2(x_\eta x_\xi + y_\xi y_\eta)\Phi_{\xi\eta} + (x_\xi^2 + y_\xi^2)\Phi_{\eta\eta}] \tag{7}$$

Therefore, Eq. (2) becomes

$$(x_\eta^2 + y_\eta^2)\Phi_{\xi\xi} - 2(x_\eta x_\xi + y_\xi y_\eta)\Phi_{\xi\eta} + (x_\xi^2 + y_\xi^2)\Phi_{\eta\eta} + J^2 k_c^2 \Phi = 0 \tag{8}$$

Equation (8) allows all computation to be done on a fixed square grid since it has been transformed so that the curvilinear coordinates replace the cartesian coordinates as the independent variables.

For the case of constant depth, substituting $\Phi = A$ $(\xi, \eta) e^{i\int k_c (J^{1/2}/\alpha) d\xi}$ into Eq. (8) yields

$$\left(\alpha A_{\xi\xi} + 2ik_c J_o^{1/2} A_\xi - \frac{k_c^2 J_o}{\alpha} A\right) - 2\beta\left(\frac{ik_c J_o^{1/2}}{\alpha} A_\eta + A_{\xi\eta}\right)$$
$$+ \gamma A_{\eta\eta} + J^2 k_c^2 A = 0 \tag{9}$$

where $\alpha = (x_\eta^2 + y_\eta^2)$, $\beta = (x_\eta x_\xi + y_\xi y_\eta)$ and $\gamma = (x_\xi^2 + y_\xi^2)$.

If the waves propagate in the propagating direction ξ, the second derivative of A with respect to ξ can be neglected as

$$2ik_c J_o^{1/2} A_\xi - 2\beta\left(\frac{ik_x J_o^{1/2}}{\alpha} A_\eta + A_{\xi\eta}\right) + \gamma A_{\eta\eta}$$

$$+ \left(J^2 - \frac{J_o}{\alpha}\right)k_c^2 A = 0 \tag{10}$$

which is the governing equation in the conformal domain. The derivatives are approximated in the finite difference form setting $\nabla\xi$ and $\nabla\eta=1$ as follows.

$$A_\xi = A_{i+1,j} - A_{i,j}$$

$$A_\eta = \frac{1}{4}(A_{i,j+1} - A_{i,j-1} + A_{i+1,j+1} - A_{i+1,j-1})$$

$$A_{\eta\eta} = \frac{1}{2}(A_{i+1,j-1} - 2A_{i+1,j} + A_{i+1,j+1})$$

$$A_{\xi\eta} = \frac{1}{2}(A_{i+1,j+1} - A_{i,j+1} - A_{i+1,j-1} + A_{i,j-1}) \tag{11}$$

Substituting into Eq. (7) yields

$$a_j A_{i,j-1} + b_j A_{i,j} + c_j A_{i,j-1} = d_{i,j} \tag{12}$$

where,

$$a_j = \left[\frac{\beta i k_c J_o^{1/2}}{2\alpha} + \beta + \frac{\gamma}{2}\right]$$

$$b_j = \left[2ik_c J_o^{1/2} - \gamma + \frac{(J^2 - J_o/\alpha)k_c^2}{2}\right]$$

$$c_j = \left[-\frac{\beta i k_c J_o^{1/2}}{2\alpha} - \beta + \frac{\gamma}{2}\right]$$

$$d_{i,j} = \left[\left(-\frac{\beta i k_c J_o^{1/2}}{2\alpha} - \frac{\gamma}{2} + \beta\right)A_{i,j-1}\right.$$

$$+ \left\{2ik_c J_o^{1/2} + \gamma - \frac{(J^2 - J_o/\alpha)k_c^2}{2}\right\}A_{i,j}$$

$$+ \left.\left(\frac{\beta i k_c J_o^{1/2}}{2\alpha} - \frac{\gamma}{2} - \beta\right)A_{i,j+1}\right] \tag{13}$$

Equation (13) can be described in a tridiagonal matrix form as

$$\begin{bmatrix} b_1 & c_1 & & & & \\ a_2 & b_2 & c_2 & & & \\ & a_3 & b_3 & c_3 & & \\ & & & \ddots & & \\ & & & & a_{ny} & b_{ny} \end{bmatrix}\begin{bmatrix} A_1 \\ A_2 \\ A_3 \\ \vdots \\ A_{ny} \end{bmatrix} = \begin{bmatrix} d_1 - a_1 \\ d_2 \\ d_3 \\ \vdots \\ d_{ny} - c_{ny} \end{bmatrix} \tag{14}$$

3.2 Hyperbolic Model

The governing equation of hyperbolic type is derived

from the mild slope Eq. (1) as a pair of first order equations as follows (Copeland, 1985).

$$\frac{Cg}{C}\frac{\partial \eta}{\partial t}+\nabla Q=0$$

$$\frac{\partial Q}{\partial t}+CCg\nabla_\eta =0 \tag{15}$$

which is similar to those used for the solutions of the shallow water equations. Equation (13) is transformed from the Cartesian $\{x, y\}$ space into an alternate $\{u, v\}$ as

$$\frac{Cg}{C}\frac{\partial \eta}{\partial t}-\frac{1}{J}(Q_{xv}y_u -Q_{xu}y_v +Q_{yu}x_v -Q_{yv}x_u)=0$$

$$\frac{\partial Q_x}{\partial t}-\frac{CCg}{J}(\eta_v y_u -\eta_u y_v)=0 \tag{16}$$

$$\frac{\partial Q_y}{\partial t}-\frac{CCg}{g}(\eta_u x_v -\eta_v x_u)=0$$

The derivatives are approximated in the finite difference form as

$$\frac{\partial \eta}{\partial t}=\frac{C}{CgJ}\{y_u (Q_{xi,j+1}-Q_{xi,j})-y_v (Q_{xi+1,j}-Q_{xi,j})$$

$$+x_v (Q_{yi+1,j}-Q_{yi,j})-x_u (Q_{yi,j+1}-Q_{yi,j})\}$$

$$\frac{\partial Q_x}{\partial t}=\frac{CCg}{J}\{y_u (\eta_{i,j+1}-\eta_{i,j})-y_v (\eta_{i+1,j}-\eta_{i,j})\} \tag{17}$$

$$\frac{\partial Q_y}{\partial t}=\frac{CCg}{J}\{x_v (\eta_{i+1,j}-\eta_{i,j})-x_u (\eta_{i,j+1}-\eta_{i,j})\}$$

This set of finite difference equations in the conformal domain is solved by the explicit scheme.

4. RESULTS

Both wave models developed here are compared for a circular channel of 4 m constant depth lying between two radii $r_1=75$ and $r_2=100$ m and covering $180°$ arc. A plane wave enters at $\theta=0$ and propagates around the bend in a counter-clockwise direction. At the downwave boundary of $\theta=180°$ the waves propagate without any reflection. The exact solution of such wave field in a circular channel was described in Dalrymple *et al.* (1994) as

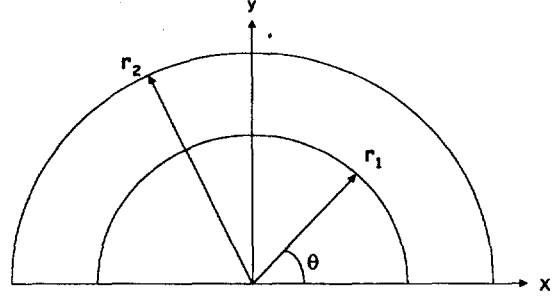$$\phi(r, \theta)=\sum_{n=0}^N a_n F_n (r)e^{i\gamma_n \theta} \tag{18}$$

Fig. 1. Schematic diagram of circular channel.

where $F_n =[Y'_{\gamma_n}(kr_1)J_{\gamma_n}(kr)-J'_{\gamma_n}(kr_1)Y_{\gamma_n}(kr)]$ with γ_n determined by satisfying

$$Y'_{\gamma_n}(kr_1)J'_{\gamma_n}(kr_2)-J'_{\gamma_n}(kr_1)Y'_{\gamma_n}(kr_2)=0, n=1, 2, \cdots N$$

to enforce a no-flux boundary condition on $r=r_1$ and $r=r_2$. The a_n values are given in the following integral form:

$$a_n =\frac{\int_{r_1}^{r_2}\phi(r, 0)r^{-1}F_n dr}{\int_{r_1}^{r_2}r^{-1}F_n^2 dr} \tag{19}$$

where the upwave boundary condition $\phi(r, 0)$ is given as 1.

To illustrate the effect of the BFCS, the parabolic and hyperbolic model results accomplished on the rectangular grid system is shown in Figs. 2(a) and 2(b), respectively and compared with the analytical solution shown in Fig. 2(c). In handling the reflecting conditions on the parabolic model, Lee and Lee's (1994) approach was employed. In the hyperbolic model, Copeland's (1985) approach was taken in order that the reflected waves travelling back pass out of the model and are not re-reflected. Each mesh is the square of 1 m $\times$ 1 m. For this case, the wavenumber k is 0.301 m^{-1}, the dimensionless channel width is $kw=37.625$ where w is the channel width. As expected, the parabolic model yields much worse results than those of hyperbolic one. Although the results of the hyperbolic model appear good as shown in Fig. 2(b), the phase error is occurred along the outer boundary as shown in Fig. 3. The model result obtained by using the BFCS are shown in Fig. 4. The numerical results show excellent similarity of the analytic solution. The reflection from the outer
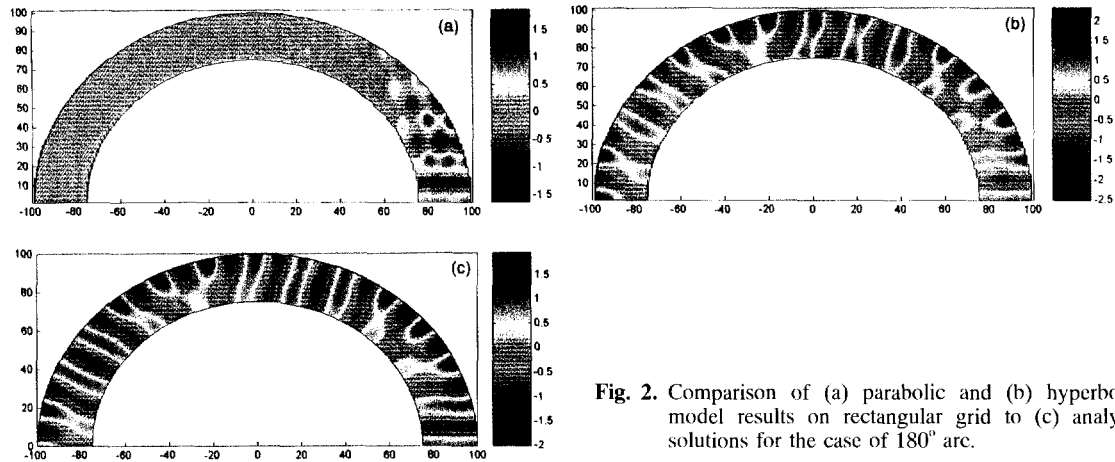
Fig. 2. Comparison of (a) parabolic and (b) hyperbolic model results on rectangular grid to (c) analytic solutions for the case of 180° arc.
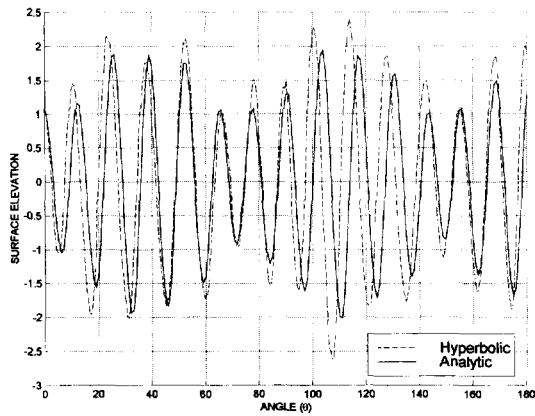

Fig. 3. Comparison of the water surface variation along outer boundary between hyperbolic model results on rectangular grid and analytic solutions for the case of 180° arc.
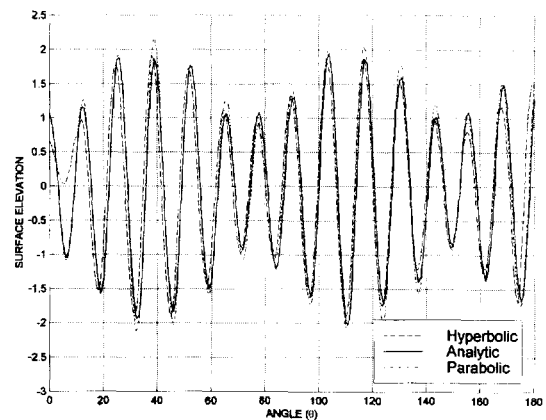

Fig. 5. Comparison of the water surface variation along outer boundary between parabolic and hyperbolic model results by BFCS and analytic solutions for the case of 180° arc.

wall is observed prominently at about 40° and 120°. For this numerical solution, the numbers of computational grids to the r and θ-directions used are n =200, m=25, respectively. Wave phases along a outer boundary are also compared in Fig. 5. All the results show good agreement when the BFCS is employed.

If waves are blocked by a cross wall at 90°, the waves take a turn in the opposite direction and propagate against a circular channel again. In the parabolic approach, differently from the iterative
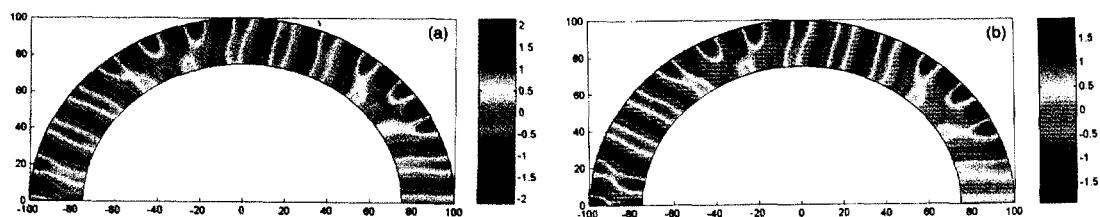

Fig. 4. Comparison of (a) parabolic and (b) hyperbolic model results by BFCS for the case of 180° arc.
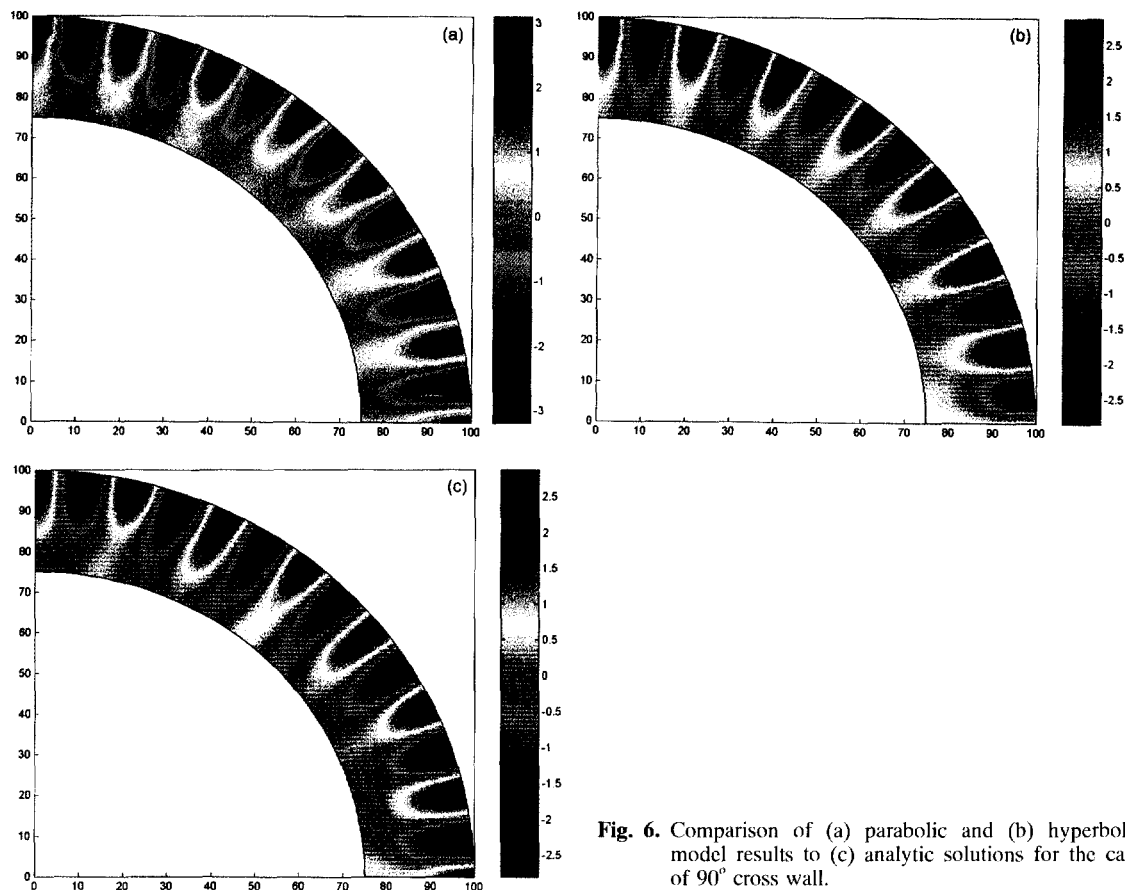
Fig. 6. Comparison of (a) parabolic and (b) hyperbolic model results to (c) analytic solutions for the case of 90° cross wall.

calculation in wave models of hyperbolic type, another backward calculation is only required in this case, and then the resulting wave field is obtained by the superposition of the foregoing waves and the waves going against a channel with reflected off the cross wall. Fig. 6 shows a comparison of the numerical results from parabolic and hyperbolic models with the analytic solutions. The analytic solution of resulting wave field can be given as

$$\phi(r,\ \theta)=\sum_{n=0}^{N}a_nF_n(r)e^{i\gamma_n\theta}+\sum_{n=0}^{N}a_nF_n(r)e^{i\gamma_n(\pi-\theta)},$$

$$0\le\theta\le\frac{\pi}{2}\tag{18}$$

5. CONCLUSIONS

Boundary-fitted coordinates have been used extensively in propagating wave fields. In this study, two wave models of hyperbolic and parabolic types have been developed through a conformal transformation. Both were compared with the analytic solutions of waves propagating through a circular channel of constant depth lying between two radii r_1=75 and r_2=100 m and covering 180° arc. Comparison indicates that both methods provide accurate results. The computation was also performed for a downwave reflecting condition. The parabolic model could also simulate the reflecting wave field by backward calculation starting with downwave conditions approaching to the wall. When a cross wall was put at 90°, the resulting wave fields obtained from both wave models were in good agreement with the exact solutions. Although the present BFCS can be directly applied to a general geometry, the present method is advisable to be

discretized by using by finite-volume method in order to yield more accurate and conservative approximation than finite difference methods.

REFERENCES

Berkhoff, J.C.W., 1972. Computation of combined refraction-diffraction, *Proc. 13th Int. Conf. Coastal Engrg., ASCE*, pp. 471-490.

Coleman, R.M., 1982. Generation of boundary-fitted coordinate systems using segmented computational regions, *Symp. on Numerical Generation of Curvilinear Coordinate Systems and Use in the Numerical Solution of Partial Differential Equations*, Nashville, Tenn., pp. 633-651.

Copeland, G.J.M., 1985. A practical alternative to the mild slope wave equation, *Coastal Eng.*, **9**, pp. 125-149.

Dalrymple, R.A. and Kirby, J.T., 1994. Waves in an annular entrance channel, *Proc. 24th Int. Conf. Coastal Engrg.*, ASCE, pp. 128-141.

Dalrymple, R.A., Suh, K.D., Kirby, J.T. and Chae, J.W., 1989. Models for very wide-angle water waves and wave diffraction. Part 2. Irregular bathymetry, *J. Fluid Mech.* **201**, pp. 299-322.

Ebersole, B.A., Cialone, M.A. and Prater, M.D., 1986. Regional coastal processes numerical modeling system, Report 1, RCPWAVE-A linear wave propagation model for engineering use, *Tech. Rep. CERC-86-4*, US Army Engineer WES, Vicksburg, Mississippi.

Kirby, J.T., 1988. Parabolic wave computation in non-orthogonal coordinate systems, *J. Waterway, Port, Coastal and Ocean Engrg.*, **114**, pp. 673-685.

Lee, J.L. and Lee, D.Y., 1994. Wave Prediction in habour by using parabolic-type numerical scheme, *Abstracts of Papers for Annual Meeting of Korean Society of Coastal and Ocean Engineers*, **6**, pp. 58-61 (in Korean).

Liu P.L.-F. and Boissevain, P.L., 1988. Wave propagation between two breakwaters, *J. Waterway, Port, Coastal and Ocean Engrg.*, **114**, pp. 237-247.

Madsen, P.A. and Larsen, J., 1987. An efficient finite-difference approach to the mild-slope equation, *Coastal Eng.*, **11**, pp. 329-351.

Melo, E. and Gobbi, M.F., 1998. Wave propagation in circular jettied channels, *J. Waterway, Port, Coastal and Ocean Engrg.*, ASCE, **124**(1), pp. 7-15.

Panchang, V.G., Cushman-Roisin, B. and Pearce, B.R., 1988. Combined refraction-diffraction of short-waves in large coastal regions, *Coastal Eng.*, **12**, pp. 133-156.

Radder, A.C., 1979. On the parabolic equation for water-wave propagation, *J. Fluid Mech.*, **95**, pp. 159-176.

Thomson, J.F., Thames, F.C. and Mastin, C.W., 1974. Automatic numerical generation of body-fitted curvilinear coordinate system for field containing any number of arbitrary two-dimensional bodies, *J. Comp. Phys.*, **15**, pp. 299-319.

Yoo, D. and O'Connor, B.A. 1986. Mathematical modeling of wave-induced nearshore circulations, *Proc. 20th Int. Conf. Coastal Engrg.*, ASCE, pp. 1667-1681.